



Semiclassical approximation meets Keldysh–Schwinger diagrammatic technique: scalar ϕ^4

A. A. Radovskaya^a , A. G. Semenov^b

P.N. Lebedev Physical Institute, 119991 Moscow, Russia

Received: 28 August 2020 / Accepted: 27 June 2021 / Published online: 6 August 2021
© The Author(s) 2021

Abstract We study the evolution of the non-equilibrium quantum fields from a highly excited initial state in two approaches: the standard Keldysh–Schwinger diagram technique and the semiclassical expansion. We demonstrate explicitly that these two approaches coincide if the coupling constant g and the Planck constant \hbar are simultaneously small. Also, we discuss loop diagrams of the perturbative approach, which are summed up by the leading order term of the semiclassical expansion. As an example, we consider shear viscosity for the scalar field theory at the leading semiclassical order. We introduce the new technique that unifies both semiclassical and diagrammatic approaches and open the possibility to perform the resummation of the semiclassical contributions.

1 Introduction

Highly nonequilibrium dense quantum fields define the initial stage of many physical problems. These include the physics of the early stage of ultrarelativistic heavy ion collisions [1–3], cold atomic gases [4,5] and the processes in the early Universe [6–11]. At present, there are a variety of approaches used for the description of the quantum field evolution from a highly excited initial state to the quasistationary one, where hydrodynamic equations work effectively.

One of the most advanced approaches is the Keldysh–Schwinger diagram technique which provides a systematic way of studying nonequilibrium phenomena in quantum field theory [3,12–14]. With the help of this technique, one can derive the kinetic equations that describe the evolution of quasiparticle distribution function and observables consequently. Also, this technique can be used for the systematic evaluation of thermodynamical and transport properties of the quantum systems at the thermal equilibrium [3,14].

Another way to deal with the nonequilibrium initial state comes from a physical intuition and is based on the assumption that at high energies and/or high occupation numbers the dynamics of the quantum fields is semiclassical, so the classical equations of motion can be used [15–25]. In order to complete this approach, one should make additional assumptions about an ensemble which is used for the averaging of observables. In the literature, this approach is often called *the Classical Statistical Approximation (CSA)*. It is very useful for numerical simulations since it allows numerically extract (nonperturbatively in coupling constant) results for observables [26–28] and transport coefficients [29]. In the previous works of one of the authors [20–22], it was shown that the CSA arises as the leading order of the semiclassical expansion.

This work aims to demonstrate that the Keldysh–Schwinger diagram technique and the classical statistical approach are two facets of one general way to deal with nonequilibrium quantum fields. It seems that these two approaches are quite different from a practical point of view. The Keldysh–Schwinger diagram technique originates from the perturbative expansion in the coupling constant g . In order to evaluate the observable consistently in this approach, one should (with the help of the Wick theorem and the diagram technique) derive the quantum kinetic equation on the distribution function, solve it, and evaluate observable using the solution. Conversely, the CSA comes from the \hbar expansion. In order to find the observable there, it is necessary to solve the classical equations of motion and to average the observable on the classical trajectories with the ensemble of the initial conditions. In this work, we show that these two approaches can be derived from one general path-integral representation. We demonstrate which assumptions and approximations should be made to obtain one approach or the other. We study the case of both g and \hbar are small, where these two approaches should be consistent, and analyse how the leading order term of the semiclassical expansion (the CSA) sums up certain

^a e-mail: raan@lpi.ru (corresponding author)

^b e-mail: semenov@lpi.ru

multi-loop diagrams of the perturbative Keldysh–Schwinger technique.

Previously some efforts were made in this direction. In particular, in works [30,31], the comparison between the Keldysh–Schwinger diagram technique and the classical approximation was performed for the thermal equilibrium, and the agreement of the leading order contributions at high temperatures was demonstrated.

The paper is organised as follows:

Starting from the general setup described in Sect. 2, we briefly review the standard Keldysh–Schwinger diagram technique in Sect. 3 and the semiclassical approximation in Sect. 4. In Sect. 5 we perform the detailed comparison of these approaches in the limit where g and \hbar are small simultaneously and analyse the loop contributions. In Sect. 6, on the example of the shear viscosity, we show how to employ the CSA for the calculation of the relevant physical observables and discuss the applicability of the semiclassical approach. Section 7 is devoted to a new diagram technique which naturally combines both approaches described above. The discussion of results and conclusions are in Sect. 8.

2 Keldysh–Schwinger approach to the non-equilibrium QFT

The standard way to deal with the non-equilibrium quantum field theory includes the Keldysh–Schwinger technique, also known as the closed-time path formalism [3,14,23]. In this approach, averages are calculated as the trace with the density matrix operator. Time evolution of the density matrix is defined by two evolution operators; that is why the doubling of the degrees of freedom occurs. Moreover, the initial density matrix should be additionally defined from the physics of the considered system.

In this work we consider the scalar field theory with the action:

$$S[\varphi(x)] = \frac{1}{2} \int d^d x \left(\partial_\mu \varphi(x) \partial^\mu \varphi(x) - m^2 \varphi^2(x) - \frac{g}{2} \varphi^4(x) \right). \quad (1)$$

Here and after we use mostly minus metric convention $g_{\mu\nu} = (+, -, -, -)$ and $x^\mu = (t, \mathbf{x})$. Using Eq. (1) one can calculate the Keldysh action as a difference between actions on the forward and the backward parts of the Keldysh contour. Averages are expressed through the path integrals with the Keldysh action as [3,14,23]:

$$\langle \hat{O} \rangle = \int \mathcal{D}\varphi_F \mathcal{D}\varphi_B O[\varphi_F, \varphi_B] e^{\frac{i}{\hbar}(S[\varphi_F] - S[\varphi_B])}. \quad (2)$$

Here and after we keep \hbar explicitly in order to study the semiclassical limit of the theory.

It is convenient to rotate the basis of φ_F, φ_B fields to the so-called “classical” and the “quantum” fields (there are equivalent notations for such rotation in the literature

$$\varphi_{cl} \equiv \varphi_r \text{ and } \varphi_q \equiv \varphi_a \text{ [3,14,23]:}$$

$$\begin{aligned} \varphi_{cl}(x) &= \frac{1}{2} (\varphi_F(x) + \varphi_B(x)), \\ \hbar \varphi_q(x) &= \varphi_F(x) - \varphi_B(x). \end{aligned} \quad (3)$$

This new φ_{cl}, φ_q basis has several advantages: the causality of the theory become explicit, the vertices look simpler, and the semiclassical limit is transparent. Then the Keldysh action transforms to (after integration by parts):

$$\begin{aligned} S[\varphi_F] - S[\varphi_B] &= S_{init}[\varphi_{cl}, \varphi_q] + S_K[\varphi_{cl}, \varphi_q], \\ S_{init}[\varphi_{cl}, \varphi_q] &= \hbar \int d^{d-1} \mathbf{x} \varphi_q(t_0, \mathbf{x}) \dot{\varphi}_{cl}(t_0, \mathbf{x}), \\ S_K[\varphi_{cl}, \varphi_q] &= -\hbar \int_{t_0}^{\infty} dt \int d^{d-1} \mathbf{x} \varphi_q(t, \mathbf{x}) \\ &\quad \times \left(\partial_t^2 - \nabla^2 + m^2 \right) \varphi_{cl}(t, \mathbf{x}) \\ &\quad - g \hbar \int_{t_0}^{\infty} dt \int d^{d-1} \mathbf{x} \left(\varphi_{cl}^3(t, \mathbf{x}) \varphi_q(t, \mathbf{x}) \right. \\ &\quad \left. + \frac{\hbar^2}{4} \varphi_{cl}(t, \mathbf{x}) \varphi_q^3(t, \mathbf{x}) \right). \end{aligned} \quad (4)$$

We keep explicit dependence on the initial time t_0 to take into account highly non-equilibrium initial states. Usually, the initial time moment is set to the past infinity, and the boundary term $S_{init}[\varphi_{cl}, \varphi_q]$ is dropped out. The averages can be calculated by integration over new fields as:

$$\langle \hat{O} \rangle = \int \mathcal{D}\varphi_{cl} \mathcal{D}\varphi_q O[\varphi_{cl}] e^{\frac{i}{\hbar} S_K[\varphi_{cl}, \varphi_q]}. \quad (5)$$

Note, if \hat{O} contains only equal-time operators, then it is sufficient to keep only the φ_{cl} component in the integrand of the expression Eq. (5) due to causality.

The expressions similar to Eqs. (5) and (2) can be found in many modern textbooks that discuss the Keldysh–Schwinger technique. However, such representation is somewhat misleading since it does not contain information about the initial state of the theory, which makes φ_F and φ_B fields correlated. More rigorously the Eq. (5) can be written as [20–22,32]:

$$\begin{aligned} \langle \hat{O} \rangle &= \int \mathcal{D}\Pi(\mathbf{x}) \mathcal{D}\alpha(\mathbf{x}) W[\alpha(\mathbf{x}), \Pi(\mathbf{x})] \\ &\quad \times \int_{i.c.} \mathcal{D}\varphi_{cl}(t, \mathbf{x}) \int \mathcal{D}\varphi_q(t, \mathbf{x}) O[\varphi_{cl}] e^{\frac{i}{\hbar} S_K[\varphi_{cl}, \varphi_q]}, \end{aligned} \quad (6)$$

where the integral with *i.c.* means the initial values for the φ_{cl} field, $\varphi_{cl}(t_0, \mathbf{x}) = \alpha(\mathbf{x})$, $\partial_t \varphi_{cl}(t_0, \mathbf{x}) = \Pi(\mathbf{x})$; whereas the initial values for the φ_q are not fixed. $S_{init}[\varphi_{cl}, \varphi_q]$ is then taken into account and absorbed by the Wigner functional.

The Wigner functional is related to the initial value of the density matrix operator $\hat{\rho}(t_0)$ as:

$$W[\alpha(\mathbf{x}), \Pi(\mathbf{x})] = \int \mathcal{D} \beta(\mathbf{x}) e^{i \int d^{d-1} \mathbf{x} \beta(\mathbf{x}) \Pi(\mathbf{x})} \times \langle \alpha(\mathbf{x}) + \frac{\hbar}{2} \beta(\mathbf{x}) | \hat{\rho}(t_0) | \alpha(\mathbf{x}) - \frac{\hbar}{2} \beta(\mathbf{x}) \rangle. \tag{7}$$

This functional contains all the information about the initial state of the system. The Eq. (6) represents the general expression from which one can deduce both the perturbative and the semiclassical approaches which were discussed in the introduction. In the next section, we derive the standard Keldysh–Schwinger perturbation technique and discuss its limitations.

3 Standard perturbative approach

The standard Keldysh–Schwinger diagram technique follows naturally from two major assumptions:

- The Gaussian form of the initial Wigner functional that allows the Wick theorem to be valid.
- The possibility of the perturbative expansion.

Under these assumptions, the Eq. (6) can be rewritten as:

$$\langle \hat{O} \rangle = \left\langle O[\varphi_{cl}] e^{-ig \int d^d x \left(\varphi_{cl}^3(x) \varphi_q(x) + \frac{\hbar^2}{4} \varphi_{cl}(x) \varphi_q^3(x) \right)} \right\rangle_0, \tag{8}$$

where the averaging over the noninteracting fields $\langle \dots \rangle_0$ should be performed with help of the Wick’s theorem with four basic contractions [3, 14, 23]:

$$\begin{aligned} \langle \varphi_{cl}(x) \varphi_{cl}(x') \rangle_0 &= i G_K^0(x; x'), \\ \langle \varphi_{cl}(x) \varphi_q(x') \rangle_0 &= i G_R^0(x; x'), \\ \langle \varphi_q(x) \varphi_{cl}(x') \rangle_0 &= i G_A^0(x; x') = i G_R^0(x'; x), \\ \langle \varphi_q(x) \varphi_q(x') \rangle_0 &= 0. \end{aligned} \tag{9}$$

Here $G_{R(A)}^0$ is retarded (advanced) Green’s functions which can be equivalently defined in the operator formalism as

$$G_R^0(x; x') = G_A^0(x'; x) = -\frac{i}{\hbar} \theta(t - t') \langle [\hat{\varphi}(x), \hat{\varphi}(x')] \rangle_0. \tag{10}$$

In the absence of the interactions these free correlators Eq. (10) are independent from the initial Wigner functional and solve the equation:

$$\hat{L}_0 G_{R(A)}^0(x; x') = -\delta^d(x - x'), \tag{11}$$

$$\hat{L}_0 = \partial_\mu \partial^\mu + m^2, \tag{12}$$

with the corresponding boundary conditions (retarded or advanced ones). The solution of the Eq. (11) is, for example:

$$G_R^0(x; x') = -\theta(t - t') \int \frac{d^{d-1} \mathbf{p}}{(2\pi)^{d-1}} \frac{\sin(\omega_p(t - t'))}{\omega_p} e^{-i\mathbf{p}(x-x')}, \quad \omega_p^2 = \mathbf{p}^2 + m^2. \tag{13}$$

The Keldysh Green’s function:

$$G_K^0(x; x') = -\frac{i}{2} \langle \{\hat{\varphi}(x), \hat{\varphi}(x')\} \rangle_0 \tag{14}$$

solves the equation:

$$\hat{L}_0 G_K^0(x; x') = 0. \tag{15}$$

This correlator depends crucially on the initial state of the system and cannot be found without specification of the initial density operator. In the simplest case, the initial state of the system is characterised by the one-particle distribution function f_p , which is related to the Keldysh Green’s function as: [3, 14, 23]

$$G_K^0(x; x') = -i\hbar \int \frac{d^{d-1} \mathbf{p}}{(2\pi)^{d-1}} \frac{\cos(\omega_p(t - t'))}{2\omega_p} \times (2f_p + 1) e^{-i\mathbf{p}(x-x')}. \tag{16}$$

It is necessary to stress here that only for the Gaussian initial state the knowledge of $G_R^0(x; x')$ and $G_K^0(x; x')$ is enough to perturbatively evaluate the average of any product of the free fields and build up the diagram technique.¹

The basic elements of each diagram are two propagators:

$$\begin{aligned} i G_R^0(x_1; x_2) & \quad x_2 \longrightarrow x_1, \\ i G_K^0(x_1; x_2) & \quad x_2 \longleftarrow x_1, \end{aligned}$$

and two vertices:

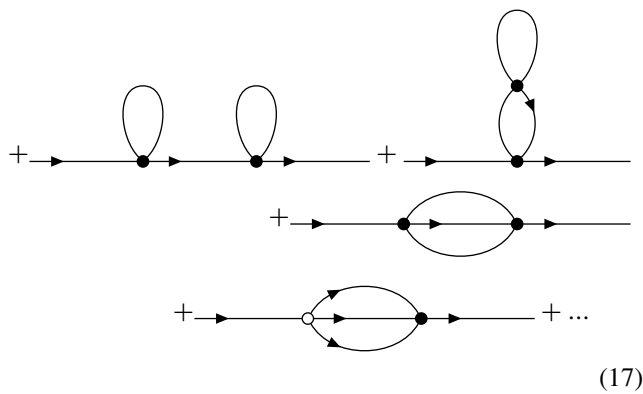
$$\begin{aligned} \text{Black vertex: } & \text{---} \bullet \text{---} \quad -ig, \\ \text{White vertex: } & \text{---} \circ \text{---} \quad -\frac{ig\hbar^2}{4}. \end{aligned}$$

Here the “black” and the “white” vertices differ by the power of \hbar^2 . It is specialised for the exact comparison with the semiclassical approach later.

For example, let us draw diagrams for the first two orders of the coupling constant expansion of the full retarded Green’s function in the presence of interactions $G_R(x, x') = -i \langle \varphi_{cl}(x) \varphi_q(x') \rangle$:

$$\text{---} \bullet \text{---} = \text{---} \bullet \text{---} + \text{---} \bullet \text{---} \text{---} \circ \text{---}$$

¹ Another way to include the initial conditions is to extend the Keldysh contour onto the imaginary axis to take into account the Matsubara part [14]. However, it works only for the special case of the thermal initial state.



and make some important observations. The first one is related to causality. The zeroth-order retarded Green’s function $G_R^0(x; x')$ is explicitly zero if $t \leq t'$. It means that time increases according to the direction of the arrow on the diagrams and each diagram in this expansion vanishes identically if $t \leq t'$. So, this diagrammatic expansion respects causality and full Green’s function $G_R(x; x') = 0$ for $t \leq t'$ as expected. The another observation, let us cut all G_K^0 lines and inspect what remains. It can be seen that the number of remaining loops exactly equal to the \hbar order of the diagram, i.e. twice of the number of the “white” vertices. We prove this statement Sect. 7. In this place, the Keldysh–Schwinger technique differs drastically from the standard Feynman diagram technique, where the \hbar order of any diagram coincides with the number of the loops.²

The notation with the arrows, which is useful for the diagrammatic, may seem somewhat misleading in calculating the number of legs with and without arrows in each vertex of a diagram. The important point is that the retarded propagator $G_R(x; x')$ connects two different fields, ϕ_{cl} and ϕ_q . The arrow in the notation belongs to the ϕ_q field (that is why arrows are moved to one end of the line in the diagrams). In order to check a diagram, it is sufficient to calculate the number of outgoing lines in each vertex. It should be either one (the black vertex) or three (the white vertex). One can find an alternative notation for this theory in the work [31].

As an example, the explicit expression for the “cactus” diagram (the last diagram on the second line of Eq. (17)) can be written:

$$G_R^{(cactus)}(x; x') = -18g^2 \int d^d y d^d y' G^R(x; y) G^R(y; y') \times G^R(y; x') G^K(y; y') G^K(y'; y'). \quad (18)$$

² For the ϕ^4 theory considered here there is an additional relation between number of the loops and number of the vertices. According to this relation, the number of the loops equal to the power of coupling constant. It comes from combinatorial arguments and valid for the Keldysh–Schwinger technique considered here.

In the next section we demonstrate how this diagram (and all others) originate from the coupling constant expansion of the CSA.

4 Semiclassical approach

In order to construct the semiclassical expansion, we add an auxiliary source $J(x)$ to the theory described by Eq. (1):

$$S[\varphi(x), J(x)] = \frac{1}{2} \int d^d x \left(\partial_\mu \varphi(x) \partial^\mu \varphi(x) - m^2 \varphi^2(x) - \frac{g}{2} \varphi^4(x) + 2J(x)\varphi(x) \right). \quad (19)$$

The source $J(x)$ is used for the intermediate steps only and should be set to zero at the end of the calculations.

Let us rewrite the Keldysh action (Eq. (4)) in a more convenient form:

$$S_K[\varphi_{cl}, \varphi_q, J] = -\hbar \int_{t_0}^{\infty} dt \int d^{d-1} \mathbf{x} \times \left(\varphi_q A[\varphi_{cl}] + \frac{g\hbar^2}{4} \varphi_{cl} \varphi_q^3 \right),$$

$$A[\varphi_{cl}] = (\partial_\mu \partial^\mu + m^2) \varphi_{cl} + g\varphi_{cl}^3 - J. \quad (20)$$

There are two key features of this action:

- $A[\varphi_{cl}] = 0$ corresponds to projecting onto the classical equation of motion of the Lagrangian (Eq. (19)).
- As far as we explicitly keep \hbar -dependence, it is clear that the semiclassical approach is, in fact, the expansion of the last term:

$$e^{-i \frac{g\hbar^2}{4} \int_{t_0}^{\infty} dt \int d^{d-1} \mathbf{x} \varphi_{cl} \varphi_q^3} = 1 - i \frac{g\hbar^2}{4} \int_{t_0}^{\infty} dt \int d^{d-1} \mathbf{x} \varphi_{cl} \varphi_q^3 + \dots \quad (21)$$

4.1 Classical statistical approximation

The Leading Order term of the semiclassical expansion (Eq. (21)) is also known as the Classical Statistical Approximation, or the classical approach. In this case, the integration over φ_q and φ_{cl} fields can be done, and the Eq. (6) reproduce the well-known result [15–22]:

$$\langle \hat{O} \rangle = \int \mathcal{D}\alpha(\mathbf{x}) \mathcal{D}\Pi(\mathbf{x}) W[\alpha(\mathbf{x}), \Pi(\mathbf{x})] O(\phi_c), \quad (22)$$

where ϕ_c is the solution of the classical equation of motion:

$$\partial_\mu \partial^\mu \phi_c + g\phi_c^3 = J \quad (23)$$

with the initial conditions given by:

$$\phi_c(t_0, \mathbf{x}) = \alpha(\mathbf{x}), \quad \partial_t \phi_c(t_0, \mathbf{x}) = \Pi(\mathbf{x}) \tag{24}$$

and at zero axillary source $J(t, \mathbf{x})$.

Hence, the recipe for the CSA is the following:

- find the classical trajectory as a function of the initial conditions.
- calculate observables on this trajectory.
- average over the initial conditions with the Wigner functional corresponding the considered problem.

Let us introduce new notation for averaging over initial conditions with the Wigner functional as:

$$\langle \dots \rangle_{i.c.} \equiv \int \mathcal{D}\alpha(\mathbf{x}) \mathcal{D}\Pi(\mathbf{x}) W[\alpha(\mathbf{x}), \Pi(\mathbf{x})] (\dots) \tag{25}$$

Then the definition of the CSA approximation (Eq. (22)) can be rewritten in this notation as

$$\langle \hat{O} \rangle = \langle O[\phi_c] \rangle_{i.c.} \tag{26}$$

It may seem that in the semiclassical expansion there are no linear in \hbar contributions. However, it is not the case since the Wigner functional may depend on the \hbar explicitly and averaging over the initial conditions may produce these terms [24,25]. For example, for the initial thermal state with the Bose distribution function and in the absence of the interactions the Kedlysh Green function, which is $G_K^0 \sim \langle \phi_c \phi_c \rangle_{i.c.}$, contains the combination (see Eq. (16)):

$$G_K^0 \sim \frac{\hbar}{\omega_p} \coth\left(\frac{\hbar\omega_p}{2T}\right).$$

In the zero temperature limit $G_K^0 \sim \hbar/\omega_p$ which is linear in \hbar , whereas for high temperature $G_K^0 \sim T/\omega_p^2$ and this contribution is purely classical and independent from \hbar .

4.2 Quantum corrections

The quantum corrections to the CSA (or the next-to-leading order of the semiclassical expansion) can be found with the help of the second term of the expansion (Eq. (21)). The integration over φ_q can not be performed straightforwardly because of the new φ_q^3 term.³ However, each φ_q can be replaced by the functional derivative over the source J due to $\varphi_q J$ term in the Keldysh action (Eq. (19)) as:

$$\varphi_q(x) e^{iS_K[\varphi_c, \varphi_q, J]} = -i \frac{\delta}{\delta J(x)} e^{iS_K[\varphi_c, \varphi_q, J]}. \tag{27}$$

³ The same problem arise during the calculation of the correlation function like $G_R(x, x')$.

Then the quantum corrections to the CSA averages are ⁴

$$\langle \hat{O} \rangle = \left\langle O[\phi_c(x)] + \frac{g\hbar^2}{4} \int dy \phi_c(y) \frac{\delta^3 O[\phi_c(x)]}{\delta J(y)^3} \Big|_{J=0} \right\rangle_{i.c.} \tag{28}$$

The recipe of Eq. (28) similar to the recipe for the CSA:

- find the classical trajectory as a function of the initial conditions.
- perform three variations over the auxiliary source (not really needed).
- integrate over intermediate time and average with the Wigner functional.

It is easy to recast all terms of the semiclassical approximation to the following general form:

$$\langle \hat{O} \rangle = \left\langle \bar{T} e^{\frac{g\hbar^2}{4} \int dy \phi_c(y) \frac{\delta^3}{\delta J^3(y)} O[\phi_c(x)]} \right\rangle_{i.c.} \tag{29}$$

Here \bar{T} denotes the anti-time ordering which is required to recover exponential form. The Eq. (29) shows that the building block of the semiclassical expansion is the full nonperturbative solution of the classical EoM $\phi_c(x)$ and its variations over the additional source $J(x)$.

It turns out that it is not necessary to calculate the variations of the classical solution explicitly. Let us define n-th variation as:

$$\Phi_n(x; x_1, x_2, \dots, x_n) = \frac{\delta^n \phi_c(x)}{\delta J(x_1) \delta J(x_2) \dots \delta J(x_n)}. \tag{30}$$

$\Phi_n(x; x_1, x_2, \dots, x_n)$ can be calculated by variation of the classical equation of motion:

$$\frac{\delta^n}{\delta J(x_1) \dots \delta J(x_n)} \left(\partial_\mu \partial^\mu \phi_c(x) + g\phi_c^3(x) = J(x) \right), \tag{31}$$

$$\begin{aligned} \hat{L}_\phi \Phi_1(x; x_1) &= \delta^{(4)}(x - x_1), \\ \hat{L}_\phi \Phi_2(x; x_1, x_2) &= -6g\phi_c(x) \Phi_1(x; x_1) \Phi_1(x; x_2), \\ \hat{L}_\phi \Phi_3(x; x_1, x_2, x_3) &= -6g\phi_c(x) \Phi_1(x; x_1) \Phi_2(x; x_2, x_3) \\ &\quad -6g\phi_c(x) \Phi_1(x; x_2) \Phi_2(x; x_1, x_3) \\ &\quad -6g\phi_c(x) \Phi_1(x; x_3) \Phi_2(x; x_1, x_2) \\ &\quad -6g\Phi_1(x; x_1) \Phi_1(x; x_2) \Phi_1(x; x_3), \end{aligned}$$

$$\dots$$

$$\hat{L}_\phi = \partial_\mu \partial^\mu + m^2 + 3g\phi_c^2(x) \equiv \hat{L}_0 + 3g\phi_c^2(x) \tag{32}$$

Hence, to calculate the quantum correction to the CSA one need to find the solution of the n coupled differential equa-

⁴ A similar \hbar^2 expansion was studied in the paper by Bödeker [24], where \hbar^2 contributions both from the initial state and the dynamical evolution were considered all together. In the later work [25] it was argued that the dynamical \hbar^2 contribution (analogous to Eq. (28)) dominates at large times.

tions without knowledge of the exact dependence of the classical solution $\phi_c(x)$ from the auxiliary source $J(x)$. The initial conditions for these equations are zero because of the causality ($\phi_c(x)$ depends on the source J only at the preceding times).

5 Comparison g^2 and \hbar^2 expansions

Now we are ready to compare the perturbative and the semiclassical approaches up to two loops. For this purpose, we perform the semiclassical expansion of the $G_R(x_1, x_2)$ up to \hbar^2 terms and show how this result, being decomposed further up to g^2 , reproduces the perturbative answer of the Sect. 3.

Let us consider the full retarded Green's function and expand it according to Eqs. (21), (27), and (30)

$$G_R(x_1, x_2) = -i \langle \phi_{cl}(x_1) \phi_q(x_2) \rangle = - \langle \Phi_1(x_1; x_2) \rangle_{i.c.} + \frac{g\hbar^2}{4} \left\langle \int dy (\Phi_1(y; x_2) \Phi_3(x_1; y, y, y) + \phi_c(y) \Phi_4(x_1; y, y, y, x_2)) \right\rangle_{i.c.} \tag{33}$$

Let us denote the Leading Order retarded Green function as $G_R^{CSA}(x_1, x_2)$, then from Eq. (33) it is obvious that

$$G_R^{CSA}(x_1, x_2) = - \langle \Phi_1(x_1; x_2) \rangle_{i.c.}, \tag{34}$$

$$\hat{L}_\phi G_R^{CSA}(x_1, x_2) = -\delta^{(d)}(x_1 - x_2). \tag{35}$$

The result of Eq. (33) presents the Leading and Next-to-Leading orders of the semiclassical expansion; however, it is still the full nonperturbative answer in the sense of the coupling constant. In order to perform expansion in g we need to express $\phi_c(x)$ and $\Phi_1(x_1; x_2)$ through the non-interacting counterparts:

$$\phi_c(x) = \phi_0(x) + g \int dy G_R^0(x, y) \phi_c^3(y),$$

$$\Phi_1(x_1; x_2) = -G_R^0(x_1, x_2) + 3g \int dy G_R^0(x_1, y) \phi_c^2(y) \Phi_1(y, x_2), \tag{36}$$

where $\phi_0(x)$ and $G_R^0(x_1, x_2)$ are solutions of the free differential equation (Eq. (11))

$$\hat{L}_0 \phi_0 = 0, \tag{37}$$

$$\hat{L}_0 G_R^0(x_1, x_2) = -\delta^{(d)}(x_1 - x_2). \tag{38}$$

The iterative expansion of the Eq. (36) up to g^2 is the following:

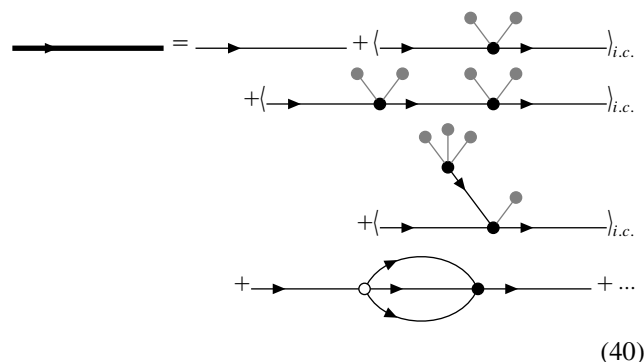
$$\begin{aligned} \phi_c(x) &= \phi_0(x) + g \int dy G_R^0(x, y) \phi_0^3(y) \\ &+ 3g^2 \int dy G_R^0(x, y) \phi_0^2(y) \\ &\times \int dz G_R^0(y, z) \phi_0^3(z) + O(g^3), \end{aligned}$$

$$\begin{aligned} \Phi_1(x_1; x_2) &= -G_R^0(x_1, x_2) \\ &- 3g \int dy G_R^0(x_1, y) \phi_0^2(y) G_R^0(y, x_2) \\ &- 9g^2 \int dy G_R^0(x_1, y) \phi_0^2(y) \\ &\times \int dz G_R^0(y, z) \phi_0^2(z) G_R^0(z, x_2) \\ &- 6g^2 \int dy G_R^0(x_1, y) \phi_0(y) G_R^0(y, x_2) \\ &\times \int dz G_R^0(y, z) \phi_0^3(z). \end{aligned} \tag{39}$$

The higher variations Φ_3 and Φ_4 can be rewritten through ϕ_c and Φ_1 with the help of the integration representations of the differential equations of Eq. (31). However, it is enough to expand the higher variation only up to g , because of the addition power of g in the second term of the Eq. (33). Moreover, the contribution of the Φ_4 vanishes, because the lowest term in this variation proportional to g^2 . The remaining \hbar^2 term of the Eq. (33) is:

$$\begin{aligned} &\frac{g\hbar^2}{4} \int dy \Phi_1(y; x_2) \Phi_3(x_1; y, y, y) \rightarrow \\ &-\frac{3g^2\hbar^2}{2} \int dy G_R^0(y, x_2) \int dz G_R^0(x_1, z) [G_R^0(z, y)]^3. \end{aligned}$$

Let us draw the contributions to the full retarded Green's function $G_R(x_1, x_2)$ pictorially.

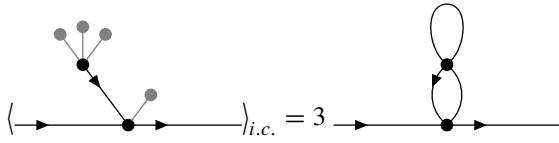


All lines and vertices have the same meaning as in Sect. 3. The only new element – the grey blob – denotes the free field $\phi_0(x)$. Since only $\phi_0(x)$ depends on the initial conditions in the above expansion, it is straightforward to perform averaging according to the rule:

$$\begin{aligned} \langle \phi_0(x) \phi_0(y) \rangle_{i.c.} &= \langle x \text{ --- } \bullet \text{ --- } y \rangle_{i.c.} \\ &= x \text{ --- } y = iG_K^0(x; y). \end{aligned} \tag{41}$$

Since we consider the Gaussian form of the Wigner functional (to satisfy the demands of the perturbative approach),

the Eq. (41) represents the basic element of the Wick’s theorem – the contraction of two $\phi_0(x)$. For example, the “cactus” diagram, that we mention earlier in Eq. (18), is recovered from the fourth term of the expansion (Eq. (5)), or the last line of Eq. (39).



All other contributions of the expansion (17) are recovered correspondingly.

One can see that the Leading Order semiclassical term (the CSA) reproduces all the contributions of the g^2 terms of the perturbative approach except the last one. However, this term is subleading for a highly occupied initial state as we discuss in the next section.

6 Shear viscosity and the CSA applicability

In this section we consider the implementation of the semiclassical formalism to the numerical simulation. The CSA is useful for numerical calculations since the path-integrals over initial conditions can be done with the help of the Monte-Carlo approach [26, 29]. Another advantage of the CSA is the possibility to take into account the strongly correlated initial conditions (non-Gaussian ones). Let us consider the shear viscosity as an example. In order to evaluate it one can use the Kubo linear response theory [29, 33–39], where transport coefficients can be expressed through the retarded correlator $R_{\alpha\beta}^{\mu\nu}$ of two components of the stress-energy tensor $T^{\mu\nu}$ as:

$$R_{\alpha\beta}^{\mu\nu}(x; x') = -\frac{i}{\hbar} \theta(t - t') \langle [\hat{T}^{\mu\nu}(x), \hat{T}_{\alpha\beta}(x')] \rangle. \tag{42}$$

The Kubo theory is valid if a system is in a (quasi)stationary state when hydrodynamical description [40] is applicable and $R_{\alpha\beta}^{\mu\nu}(x; x')$ depends only on $x - x'$. In the rest frame, the shear viscosity can be expressed through the Fourier transform of the (12–12) correlation function:

$$R_{12}^{12}(p) = \int d^4(x - x') e^{ip^\mu(x_\mu - x'_\mu)} R_{12}^{12}(x; x')$$

as:

$$\eta = i \lim_{p^0 \rightarrow 0} \lim_{p^i \rightarrow 0} \partial_0 R_{12}^{12}(p). \tag{43}$$

However, for the real physical systems, it is useful to consider the shear viscosity in the general frame where the energy flow can exist. One can define the flow velocity u^μ for energy current as the only time-like eigenvector of the average stress-energy tensor $\langle \hat{T}^{\mu\nu} \rangle$ with eigenvalue equal to energy density ε . We normalize the flow velocity as $u_\mu u^\mu = 1$. In this case, one can rewrite the expression for shear viscosity in the

covariant form through the retarded correlator of the traceless part of the stress tensor. The final expression is:

$$\eta(x) = -\frac{1}{10} \Delta_{\alpha\beta}^{\mu\nu} \int d^4y u^\rho y_\rho R_{\mu\nu}^{\alpha\beta}(x + y; x), \tag{44}$$

where:

$$\Delta_{\alpha\beta}^{\mu\nu} = \frac{1}{2} \left(\Delta_\alpha^\mu \Delta_\beta^\nu + \Delta_\alpha^\nu \Delta_\beta^\mu - \frac{2}{3} \Delta^{\mu\nu} \Delta_{\alpha\beta} \right),$$

$$\Delta^{\mu\nu} = g^{\mu\nu} - u^\mu u^\nu.$$

The Eq. (44) describes the quasistationary state where the viscosity can be a slow function of the space-time point x , rather than the constant value of Eq. (43). It is likely to obtain such a physical system in the later stages of the nonequilibrium matter evolution. Moreover, the Eq. (44) allows evaluation of the shear viscosity in the system with the nonzero energy flow without transformation to the rest frame of the medium.

Note that the Eq. (44) can be considered as the shear viscosity only in the range of validity of the hydrodynamic description. For the correlator of the Eq. (44) it means that $\Delta_{\mu\nu}^{\alpha\beta} R_{\alpha\beta}^{\mu\nu}(x + y; x)$ weakly changes as a function of x and fast decays as a function of y . In other words, all the microscopic dynamics should enter into the large scale behaviour only through the number of the transport coefficients.

For the system under consideration the stress energy tensor equals to:

$$T^{\mu\nu} = \partial^\mu \varphi \partial^\nu \varphi - g^{\mu\nu} \left(\frac{1}{2} \partial^\rho \varphi \partial_\rho \varphi - \frac{1}{2} m^2 \varphi^2 - \frac{g}{4} \varphi^4 \right), \tag{45}$$

and only the first part $\Theta^{\mu\nu}(x) = \partial^\mu \varphi(x) \partial^\nu \varphi(x)$ contribute to the shear viscosity. It means that we need to evaluate retarded correlator which is proportional to $\langle \Theta_{cl}^{\mu\nu}(x) \Theta_q^{\alpha\beta}(x') \rangle$ where the definition of the “classical” and the “quantum” components are the same as before:

$$\Theta_{cl}^{\mu\nu}(x) = \frac{1}{2} (\Theta_F^{\mu\nu}(x) + \Theta_B^{\mu\nu}(x))$$

$$\hbar \Theta_q^{\mu\nu}(x) = \Theta_F^{\mu\nu}(x) - \Theta_B^{\mu\nu}(x).$$

In terms of $\varphi_{cl(q)}$ the result is:

$$R(x; x') \equiv \Delta_{\mu\nu}^{\alpha\beta} R_{\alpha\beta}^{\mu\nu}(x; x')$$

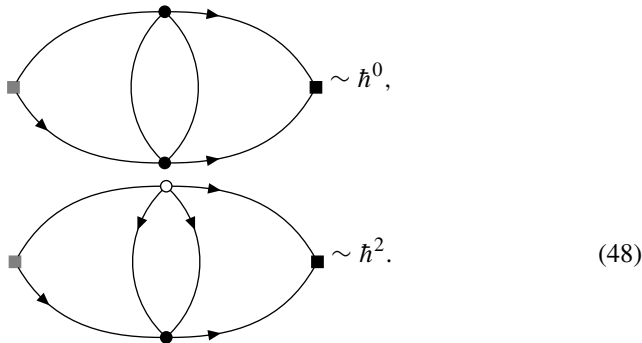
$$= -2i \Delta_{\mu\nu}^{\alpha\beta} \langle \partial^\mu \varphi_{cl}(x) \partial^\nu \varphi_{cl}(x) \partial'_\alpha \varphi_{cl}(x') \partial'_\beta \varphi_q(x') \rangle, \tag{46}$$

where $\partial'_\alpha = \frac{\partial}{\partial x'^\alpha}$. Now we can apply the semiclassical approach and derive the leading order contribution for $R(x; x')$. We obtain the CSA answer:

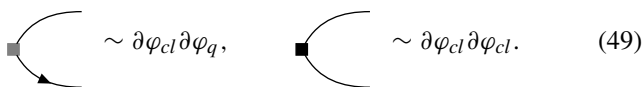
$$R(x; x') = -4 \Delta_{\mu\nu}^{\alpha\beta} \langle \partial^\mu \phi_c(x) \partial'_\alpha \phi_c(x') \partial^\nu \partial'_\beta \Phi_1(x; x') \rangle_{i.c.} \tag{47}$$

Here $\phi_c(x)$ is the solution of the classical EoM and $\Phi_1(x; x')$ – the solution of the linear differential equation (32). The averaging over the initial conditions $\langle \dots \rangle_{i.c.}$ is done with the Wigner functional Eq. (25) defined by a physical problem under consideration. The dynamics in this approximation is classical; the only \hbar – corrections can be obtained from the Wigner functional.

In principle, by taking variational derivatives of the Eq. (47), one can obtain the next-to-leading order semiclassical terms (\hbar^2) or the quantum corrections to the CSA. Another way to obtain these quantum corrections is to use the technique described in Sect. 7 below. Let us explicitly consider the two similar diagrams Eq. (48) which are included to the Eq. (46). The first diagram contributes to the leading order shear viscosity, and it is taken into account by the CSA, whereas the second one proportional to \hbar^2 and belongs to the NLO semiclassical term.



Here the squared vertices arise from the value we consider – the shear viscosity Eq. (46) as:



One can observe that the difference in (48) comes only from the central loop. In the first case, it contains the product of two Keldysh Green functions $\sim G_K^0 G_K^0$, whereas the second one has $\sim G_R^0 G_R^0$ insertion. Every Keldysh Green function has $2f_p + 1$ multiplier in contrast to the retarded one (see Eqs. (16), (13)). If the initial state is highly occupied (i.e. the system is almost classical), then $f_p \gg 1$, and we can neglect the second contribution. This analysis can be extended to any diagram, contributing to the viscosity or any other observable. For each diagram $\sim \hbar^{2n}$ there is the diagram $\sim \hbar^0$ which differs by $2n$ times substitutions of G_R^0 by G_K^0 . In other words, in this diagram n “white” vertices are changed to the “black” ones. The resulting diagram is greater due to $2f_p + 1$ factors and is already included in the CSA. It explains why the CSA works well for the highly excited initial state and sums up all leading contributions. Hence, the results of works [27,31] are clarified.

7 \hbar^2 diagram technique

In previous sections, we consider two different approaches. The first one is the Keldysh–Schwinger diagram technique with two propagators $G_{R/K}(x, x')$ and two vertices as building blocks. The other one is the semiclassical approach where the main objects are the classical solution $\phi_c(x)$ and the classical response functions $\Phi_n(x; x_1, \dots, x_n)$ for a given initial condition. In order to obtain observables in the latter approach, one should perform the averaging over all possible initial conditions. In Sect. 5, we show that both approaches are equivalent for small g and \hbar . Also, we demonstrate that the leading contributions of the semiclassical expansion (the CSA) represent a sum of an infinite number of diagrams in the perturbative approach. In this section, we develop a new approach that combines the advantages of both the CSA and the diagram technique and permits systematic improvement of the CSA and analysis of the higher-order quantum corrections. Let us start again from the general expression for the some observable (Eq. (6)) and shift the integration variable $\varphi_{cl}(x) = \phi_c(x) + \tilde{\varphi}_{cl}(x)$, where $\phi_c(x)$ is the solution of the classical equation of motion with the corresponding boundary conditions. After that $\tilde{\varphi}_{cl}$ obeys zero boundary conditions and all dependence of $\alpha(\mathbf{x})$ and $\Pi(\mathbf{x})$ enters into the path integral only through $\phi_c(x)$. This trick can be done for any quantity of interest. For example, the full retarded Green’s function can be represented as:

$$G_R(x; x') = -i \left\langle \int_{\text{zero i.c.}} \mathcal{D}\tilde{\varphi}_{cl} \int \mathcal{D}\varphi_q \tilde{\varphi}_{cl}(x)\varphi_q(x') \times e^{-i \int d^d x (\varphi_q(x) \hat{L}_\phi \tilde{\varphi}_{cl}(x) + 3g\phi_c(x)\tilde{\varphi}_{cl}^2(x)\varphi_q(x) + g\tilde{\varphi}_{cl}^3(x)\varphi_q(x))} \times e^{-i \frac{g\hbar^2}{4} \int d^d x (\phi_c(x)\varphi_q^3(x) + \varphi_{cl}(x)\varphi_q^3(x))} \right\rangle_{i.c.} \quad (50)$$

Now we perform the perturbative expansion of the above expression (without averaging over the initial conditions yet). One can check that due to the zero initial conditions for $\tilde{\varphi}_{cl}$ there is only one non-zero contraction:

$$\langle \langle \tilde{\varphi}_{cl}(x)\varphi_q(x') \rangle \rangle = -i\Phi_1(x; x'). \quad (51)$$

Here, by double angle brackets $\langle \langle \dots \rangle \rangle$ we denote the functional integration without averaging over the initial conditions. This contraction is represented by the dashed line in diagrams:

$$x' \text{-----} \rightarrow \text{-----} x \quad - i\Phi_1(x; x').$$

The “price” for the absence of the $\langle \langle \tilde{\varphi}_{cl}\tilde{\varphi}_{cl} \rangle \rangle$ propagator is the presence of four different vertices in the theory:

the value of $\phi_c(x)$ at a given space-time point is also random in some sense. Therefore, one can think of $\phi_c(x)$ as of some noisy background fluctuating in space and time. At the same time the equation for $\Phi_1(x; x')$

$$\left(\hat{L}_0 + 3g\phi_c^2(x)\right) \Phi_1(x; x') = -\delta^{(4)}(x - x') \quad (57)$$

describes the retarded propagator for a scalar particle in that noisy background. It looks similar to the Langevine equation for a Brownian particle interacting with the environment (see, for example, [42] and references therein). However, here noise is generated not by external bath as in the case of Brownian particle but by the scalar field itself. From this point of view, vertices in our diagrammatic technique correspond to the creation or annihilation of additional scalar particles. Contribution from each event of a particle creation contains an additional small \hbar^2 factor. It means that in the semiclassical limit, only contribution from noisy background survives, and the CSA works well.

8 Conclusions

In this work, we compare two approaches to the descriptions of the nonequilibrium quantum scalar fields:

- The standard Keldysh–Schwinger diagram technique, which requires the Gaussian initial conditions and the small coupling constant.
- The semiclassical expansion, which works with the arbitrary coupling constant, but valid for highly excited (or highly occupied) initial states only.

We analyse these two expansions at the limit where the coupling constant g and the Planck constant \hbar are simultaneously small. We prove the consistency of these approaches and explicitly demonstrate that already the first term of the semiclassical expansion (the Classical Statistical Approximation) includes almost all two loop-diagrams of the standard perturbative approach. We show that the only remaining $g^2\hbar^2$ diagram is small if the initial conditions are overoccupied i.e. the one-particle distribution function $f_p \gg 1$. In practice, this condition defines the applicability of the CSA.

As an example of the usefulness of the semiclassical approach, we evaluate the shear viscosity in a more general case of nonzero energy flow.

Also, we present a new diagram technique that combines both the advantages of the semiclassical and the Keldysh–Schwinger diagrammatic approaches. We believe that this technique allows to perform the resummation of the next-to-leading order semiclassical contributions and to improve the CSA.

Acknowledgements This work was supported by the RFBR project 18-02-40131.

Data Availability Statement This manuscript has no associated data or the data will not be deposited. [Authors' comment: This work does not contain experimental data.]

Open Access This article is licensed under a Creative Commons Attribution 4.0 International License, which permits use, sharing, adaptation, distribution and reproduction in any medium or format, as long as you give appropriate credit to the original author(s) and the source, provide a link to the Creative Commons licence, and indicate if changes were made. The images or other third party material in this article are included in the article's Creative Commons licence, unless indicated otherwise in a credit line to the material. If material is not included in the article's Creative Commons licence and your intended use is not permitted by statutory regulation or exceeds the permitted use, you will need to obtain permission directly from the copyright holder. To view a copy of this licence, visit <http://creativecommons.org/licenses/by/4.0/>.
Funded by SCOAP³.

References

1. F. Gelis, Int. J. Mod. Phys. E **24**(10), 1530008 (2015). https://doi.org/10.1142/9789814663717_0002
2. A. Kurkela, Nucl. Phys. A **956**, 136 (2016). <https://doi.org/10.1016/j.nuclphysa.2016.01.069>
3. J. Berges, (2015). arXiv preprint [arXiv:1503.02907](https://arxiv.org/abs/1503.02907)
4. J. Berges, T. Gasenzer, Phys. Rev. A **76**(3), 033604 (2007). <https://doi.org/10.1103/physreva.76.033604>
5. K.L. Lee, N.P. Proukakis, J. Phys. B At. Mol. Opt. Phys. **49**(21), 214003 (2016). <https://doi.org/10.1088/0953-4075/49/21/214003>
6. D.T. Son, (1996). arXiv preprint, [arXiv:hep-ph/9601377](https://arxiv.org/abs/hep-ph/9601377)
7. S.Y. Khlebnikov, I.I. Tkachev, Phys. Rev. Lett. **77**(2), 219 (1996). <https://doi.org/10.1103/physrevlett.77.219>
8. D. Boyanovsky, Phys. Rev. D **92**(2), 023527 (2015). <https://doi.org/10.1103/physrevd.92.023527>
9. E.T. Akhmedov, H. Godazgar, F.K. Popov, Phys. Rev. D **93**(2), 024029 (2016). <https://doi.org/10.1103/physrevd.93.024029>
10. E.T. Akhmedov, F. Bascone, Phys. Rev. D **97**(4), 045013 (2018). <https://doi.org/10.1103/physrevd.97.045013>
11. A. Arrizabalaga, J. Smit, A. Tranberg, J. High Energy Phys. **2004**(10), 017 (2004). <https://doi.org/10.1088/1126-6708/2004/10/017>
12. L.V. Keldysh, Sov. Phys. JETP **20**(4), 1018 (1965)
13. J. Schwinger, J. Math. Phys. **2**(3), 407 (1961). https://doi.org/10.1007/978-94-009-9426-3_22
14. J. Ghiglieri, A. Kurkela, M. Strickland, A. Vuorinen, (2020). arXiv preprint [arXiv:2002.10188](https://arxiv.org/abs/2002.10188)
15. S. Mrówczyński, B. Müller, Phys. Rev. D **50**(12), 7542 (1994). <https://doi.org/10.1103/physrevd.50.7542>
16. K. Fukushima, F. Gelis, L. McLerran, Nucl. Phys. A **786**(1–4), 107 (2007). <https://doi.org/10.1016/j.nuclphysa.2007.01.086>
17. K. Dusling, T. Epelbaum, F. Gelis, R. Venugopalan, Nucl. Phys. A **850**(1), 69 (2011). <https://doi.org/10.1016/j.nuclphysa.2010.11.009>
18. T. Epelbaum, F. Gelis, Nucl. Phys. A **872**(1), 210 (2011). <https://doi.org/10.1016/j.nuclphysa.2011.09.019>
19. K. Dusling, T. Epelbaum, F. Gelis, R. Venugopalan, Phys. Rev. D **86**(8), 085040 (2012). <https://doi.org/10.1103/physrevd.86.085040>
20. A.V. Leonidov, A.A. Radovskaya, JETP Lett. **101**(4), 215 (2015). <https://doi.org/10.1134/s0021364015040104>

21. A.V. Leonidov, A.A. Radovskaya, in *EPJ Web of Conferences*, vol. 125 (EDP Sciences, 2016), vol. 125, p. 05013. <https://doi.org/10.1051/epjconf/201612505013>
22. A.V. Leonidov, A.A. Radovskaya, *Eur. Phys. J. C* **79**(1), 55 (2019). <https://doi.org/10.1140/epjc/s10052-019-6586-x>
23. S. Jeon, *Ann. Phys.* **340**(1), 119 (2014). <https://doi.org/10.1016/j.aop.2013.09.019>
24. D. Bödeker, *Nucl. Phys. B* **486**(1–2), 500 (1997). [https://doi.org/10.1016/S0550-3213\(96\)00688-8](https://doi.org/10.1016/S0550-3213(96)00688-8)
25. D. Bödeker, M. Laine, O. Philipsen, *Nucl. Phys. B* **513**(1–2), 445 (1998). [https://doi.org/10.1016/S0550-3213\(98\)00696-8](https://doi.org/10.1016/S0550-3213(98)00696-8)
26. K. Boguslavski, A. Kurkela, T. Lappi, J. Peuron, *Phys. Rev. D* **98**(1), 014006 (2018). <https://doi.org/10.1103/physrevd.98.014006>
27. G. Aarts, *Phys. Lett. B* **518**(3–4), 315 (2001). [https://doi.org/10.1016/S0370-2693\(01\)01081-4](https://doi.org/10.1016/S0370-2693(01)01081-4)
28. G. Aarts, J. Berges, *Phys. Rev. Lett.* **88**(4), 041603 (2002). <https://doi.org/10.1103/PhysRevLett.88.041603>
29. M. Homor, A. Jakovac, *Phys. Rev. D* **92**(10), 105011 (2015). <https://doi.org/10.1103/physrevd.92.105011>
30. G. Aarts, J. Smit, *Phys. Lett. B* **393**(3–4), 395 (1997). [https://doi.org/10.1016/S0370-2693\(96\)01624-3](https://doi.org/10.1016/S0370-2693(96)01624-3)
31. G. Aarts, J. Smit, *Nucl. Phys. B* **511**(1–2), 451 (1998). [https://doi.org/10.1016/S0550-3213\(97\)00723-2](https://doi.org/10.1016/S0550-3213(97)00723-2)
32. D. Horváth, I. Lovas, M. Kormos, G. Takács, G. Zaránd, *Phys. Rev. A* **100**(1), 013613 (2019). <https://doi.org/10.1103/physreva.100.013613>
33. R. Kubo, *J. Phys. Soc. Jpn.* **12**(6), 570 (1957). <https://doi.org/10.1143/jpsj.12.570>
34. A. Hosoya, M.A. Sakagami, M. Takao, *Ann. Phys.* **154**(1), 229 (1984). [https://doi.org/10.1016/0003-4916\(84\)90144-1](https://doi.org/10.1016/0003-4916(84)90144-1)
35. S. Jeon, *Phys. Rev. D* **52**(6), 3591 (1995). <https://doi.org/10.1103/physrevd.52.3591>
36. A. Jakovac, *Phys. Lett. B* **446**(3–4), 203 (1999). [https://doi.org/10.1016/S0370-2693\(98\)01496-8](https://doi.org/10.1016/S0370-2693(98)01496-8)
37. E. Wang, U. Heinz, X. Zhang, *Phys. Rev. D* **53**(10), 5978 (1996). <https://doi.org/10.1103/physrevd.53.5978>
38. E. Wang, U. Heinz, *Phys. Lett. B* **471**(2–3), 208 (1999). [https://doi.org/10.1016/S0370-2693\(99\)01324-6](https://doi.org/10.1016/S0370-2693(99)01324-6)
39. A. Czajka, S. Jeon, *Phys. Rev. C* **95**(6), 064906 (2017). <https://doi.org/10.1103/physrevc.95.064906>
40. S. Jeon, U. Heinz, *Int. J. Mod. Phys. E* **24**(10), 1530010 (2015). https://doi.org/10.1142/9789814663717_0003
41. Z.G. Mou, P.M. Saffin, A. Tranberg, S. Woodward, J. High Energy Phys. **2019**, 6 (2019). [https://doi.org/10.1007/jhep06\(2019\)094](https://doi.org/10.1007/jhep06(2019)094)
42. J.T. Hsiang, B.L. Hu, *Phys. Rev. D* **101**(12), 125003 (2020). <https://doi.org/10.1103/PhysRevD.101.125003>